

Evaluation and Improvements to the Aeroprediction Code Based on Recent Test Data

F. G. Moore,^{*} R. M. McInvile,[†] and T. C. Hymer[‡]
U.S. Naval Surface Warfare Center, Dahlgren, Virginia 22448-5100

The 1998 (AP98) and prior versions of the U.S. Naval Surface Warfare Center, Dahlgren Division Aeroprediction Code are based primarily on slender body and perturbation theories at low angle of attack and empirical constants that represent the nonlinear aerodynamics as a function of angle of attack, Mach number, aspect and taper ratio, and other missile geometric parameters. The primary database on which these empirical nonlinear constants were derived was based on the NASA/Tri-Service component database taken in the 1970s. This database was limited in body radius to wing semispan plus body radius ratios of 0.5. A more recent database taken by NASA and the former McDonnell Douglas Corporation investigated other values of the parameter: body radius to wing semispan plus body radius ratio of 0.25, 0.33, and 0.5. As a result of this new database, the empirical constants in the AP98 that represent many of the aerodynamic nonlinearities were fine tuned. This fine tuning, along with other minor improvements, has shown the average normal force coefficient errors to be reduced by anywhere from 10 to over 40% on various missile configurations. The largest reductions in error were for configurations where the AP98 average accuracy was the worst. These new improved empirical constants will be a part of the next planned release of the aeroprediction code in 2002 (AP02). The AP98 average error on normal force coefficient of $\pm 10\%$ will, therefore, be somewhat better for the AP02.

Nomenclature

A	= planform area of wing in crossflow plane, ft^2	c_r	= root chord, ft
A_P	= planform area of body in crossflow plane, ft^2	c_t	= tip chord, ft
\mathcal{A}	= aspect ratio, b^2/A_w	K	= generic interference factor
A_{ref}	= reference area (maximum cross-sectional area of body, if a body is present, or planform area of wing, if wing alone), ft^2	$K_{B(W)}$, $K_{B(T)}$	= ratio of additional body normal-force coefficient in presence of wing, or tail-to-wing or tail-alone normal-force coefficient at $\delta=0$ deg
b	= wing span (not including body), ft	$K_{W(B)}$, $K_{T(B)}$	= ratio of normal-force coefficient of wing or tail in presence of body to that of wing or tail alone at $\delta=0$ deg
C_A	= axial force coefficient	$k_{B(W)}$, $k_{B(T)}$	= ratio of additional body normal-force coefficient due to presence of wing or tail at a control deflection to that of wing or tail alone at $\alpha=0$ deg
C_{d_c}	= crossflow drag coefficient	$k_{W(B)}$, $k_{T(B)}$	= ratio of wing or tail normal-force coefficient in presence of body due to a control deflection to that of wing or tail alone at $\alpha=0$ deg
C_M	= pitching moment coefficient (based on reference area and body diameter, if body present, or mean aerodynamic chord, if wing alone; can be about nose or center of gravity location)	M_N	= Mach number normal to body, $M_\infty \sin \alpha$
C_{M_B}	= pitching moment coefficient of body alone	M_{N_C}	= normal Mach number where flow transitions from subcritical to supercritical conditions
C_N	= normal force coefficient	M_∞	= freestream Mach number
C_{N_B}	= normal force coefficient of body alone	Re	= Reynolds number
$C_{N_B(V)}$	= negative afterbody normal-force coefficient due to canard or wing-shed vortices	Re_C	= Reynolds number where flow transitions from subcritical to supercritical conditions
C_{N_L}	= linear component of normal-force coefficient	r	= local body radius, ft
C_{N_NL}	= nonlinear component of normal-force coefficient	r_w, r_T	= radius of body at wing or tail locations
$C_{N_T(V)}$	= negative normal-force coefficient component on tail due to wing or canard-shed vortex	s	= wing or tail semispan plus the body radius in wing-body lift methodology
C_{N_W}	= normal force coefficient of wing alone	x_{CP}	= center of pressure (in feet or calibers from some reference point that can be specified) in x direction
C_{N_α}	= normal-force coefficient derivative	$(x_{\text{CP}})_L$, $(x_{\text{CP}})_{\text{NL}}$	= center of pressure of linear and nonlinear terms of normal force
$(C_{N_\alpha})_W$, $(C_{N_\alpha})_T$	= normal-force coefficient slope of wing and tail, respectively	x, y, z	= axis system fixed with x along centerline of body
		α	= angle of attack, deg
		ΔK	= nonlinear component of wing-body or body-wing interference
		δ	= control deflection deg, positive leading edge up
		η	= parameter used in viscous crossflow theory for nonlinear body normal force (in this context, it is the normal force of a circular cylinder of given length-to-diameter ratio to that of a cylinder of infinite length)
		η_0	= value of η at $M_N = 0$
		Λ_{LE}	= leading-edge sweep angle of fin, deg

Received 19 December 1999; accepted for publication 8 May 2000. This material is declared a work of the U.S. Government and is not subject to copyright protection in the United States.

We announce with regret that Roy McInvile, the second author on this paper, passed away on 11 November 1999 after being diagnosed with cancer earlier in the summer. Roy has been instrumental in the aeroprediction technology development effort for the past 10 years or so. We will sorely miss him as a friend, technical collaborator, and coworker, as will many of his friends in the technical community.

*Senior Aerodynamicist, Weapons Systems Department, Dahlgren Division. Associate Fellow AIAA.

[†]Aerospace Engineer (deceased 11 November 1999), Weapons Integration Branch, Weapons Systems Department, Dahlgren Division.

[‡]Aerospace Engineer, Aeromechanics Branch, Weapons Systems Department, Dahlgren Division.

λ	= taper ratio of a lifting surface, c_t/c_r
Φ	= roll position of missile fins ($\Phi = 0$ deg corresponds to fins in the plus + orientation, $\Phi = 45$ deg corresponds to fins rolled to the cross \times orientation)

Subscripts

c, d, t, w	= canard, dorsal, tail, and wing, respectively
--------------	--

Introduction

THE 1998 version of the U.S. Naval Surface Warfare Center, Dahlgren Division Aeroprediction Code (AP98)¹ is the most complete and comprehensive semiempirical code produced to date by the authors. It includes the capability to predict planar aerodynamics in the roll positions of $\Phi = 0$ deg (fins in + or plus orientation as viewed from the rear of the missile) and $\Phi = 45$ deg (fins in \times or cross roll orientation as viewed from the rear of the missile) over a broad range of flight conditions and configuration geometries with good average accuracy, computational times, and ease of use. Flight conditions include angles of attack (AOA) up to 90 deg, control deflections of up to ± 30 deg, and Mach numbers up to 20. Configuration geometries (Fig. 1) include axisymmetric and nonaxisymmetric body shapes with sharp, blunt, or truncated nose tips, with or without a boattail or flare. Up to two sets of planar or cruciform fins are allowed. New technology has recently been developed² to allow both six- and eight-fin options in the fin considerations as well.

Average accuracies are $\pm 10\%$ for normal and axial force and $\pm 4\%$ of body length for center of pressure. By average accuracy, it is meant that enough AOA or Mach numbers are considered to get a good statistical sample. On occasion, a single data point can exceed these average accuracy values. Ease of use has been significantly enhanced over older versions of the aeroprediction code (APC) through a personal-computer-based pre- and postprocessor package.³ This package has allowed inputs for configuration geometries to be simplified significantly by many automated nose shape options.

The semiempirical model for the wing and wing-body interference aerodynamics of the AP98 was based primarily on missile component databases^{4–6} where the parameter r/s was a constant value of 0.5 (see Fig. 1 for nomenclature). More recently, a new missile component database has been made available⁷ where data were measured for wing-alone and wing-body configurations with $r/s = 0.25, 0.33$, and 0.5 . This new database should, therefore, allow refinements in the AP98 methodology for the wing alone as well as for the effects due to r/s . It is, therefore, the purpose of this paper to first compare the AP98 predictions of normal force coefficient and center of pressure to the Ref. 7 database; secondly, to define areas of possible improvement in the AP98; and, thirdly, to refine the nonlinear aerodynamic methods in the AP98 in the areas where predictions are the weakest. These new refinements will be made a part of the next version of the APC transitioned to users, which will be the AP02 in fiscal year 2002.

The work that was performed and is the subject of this paper is presented in detail in Ref. 8. For those interested in seeing more comparisons of the AP98 and improvements made to the AP98 (AP02) compared to data, Ref. 8 should be consulted.

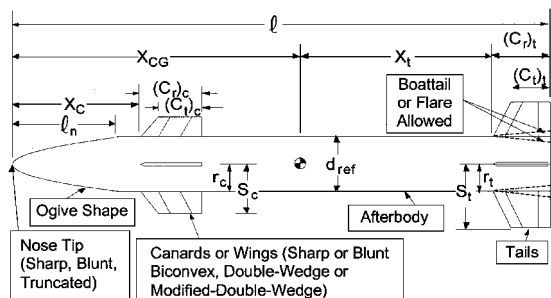


Fig. 1 Typical axisymmetric weapon configuration geometry options and nomenclature.

AP98 Comparisons to NASA/McDonnell Douglas (NASA/MDAC) Database

Figure 2 shows a scaled model comparison of the NASA Tri-Service database⁴ configurations on which the nonlinear aerodynamic terms of the AP98 were primarily based and the more recent NASA/McDonnell Douglas (NASA/MDAC) database configuration, which is the subject of this paper. In comparing the Ref. 4 and 7 models and databases, several points are worthy of note. First, the wind tunnels used in Ref. 4 were the supersonic tunnel at NASA Langley Research Center and the subsonic facility at NASA Ames Research Center, whereas the tunnels used in Ref. 7 were both at NASA Langley Research Center. The supersonic tunnel was the same as that of Ref. 4, but the transonic and subsonic data were from the NASA Langley Research Center, 8-ft transonic facility. Second, the Mach number range of Ref. 4 was from 0.6 to 4.6, whereas that of Ref. 7 was from 0.6 to 3.95. Third, the AOA range of Ref. 4 was from 0 to 40, whereas the range of Ref. 7 was from 0 to 25 to 30 deg, depending on the Mach number. The nose shape of both bodies were identical, but the Ref. 7 tests had an afterbody length 1 in. shorter than that of Ref. 4. Hence, Ref. 4 data are for a 12.33-caliber body and Ref. 7 data are for a 12.0-caliber body. The single wing planform areas of the Ref. 4 database that were tested in conjunction with the body varied in area from 1.125 in.² to 18 in.², whereas those of Ref. 7 varied in area from 2.25 in.² to 20.25 in.². However, the largest fin of Ref. 4 was for aspect ratio of 0.25 and the database was not complete. Hence, effectively, the wing area of the Ref. 4 data varied from 1.125 to 9 in.², so that, in effect, the wing sizes of the Ref. 7 data were about twice the size of those tested in Ref. 4. Another major difference was that the wing-alone data used in the AP98 were based primarily on Refs. 5 and 9. The Ref. 5 data were taken using a sting mount in the tunnel and integrated pressure data. Although it is believed that the wing-alone database of Ref. 5 could be slightly low in some cases because of thickness effects, the authors believe this is the best wing-alone database available. The Ref. 7 data for wing-alone aerodynamics was taken based on the same wings of Fig. 2 that were tested on the body alone, in contrast to the Refs. 4 and 5 data, where different size wings were tested for wing alone and wing in conjunction with the body data (because of requirements for many pressure taps in the wing-alone measurements). The wing-alone data of Ref. 7 were obtained on a splitter plate, vs a sting in the Ref. 5 data, and, as will be discussed later,

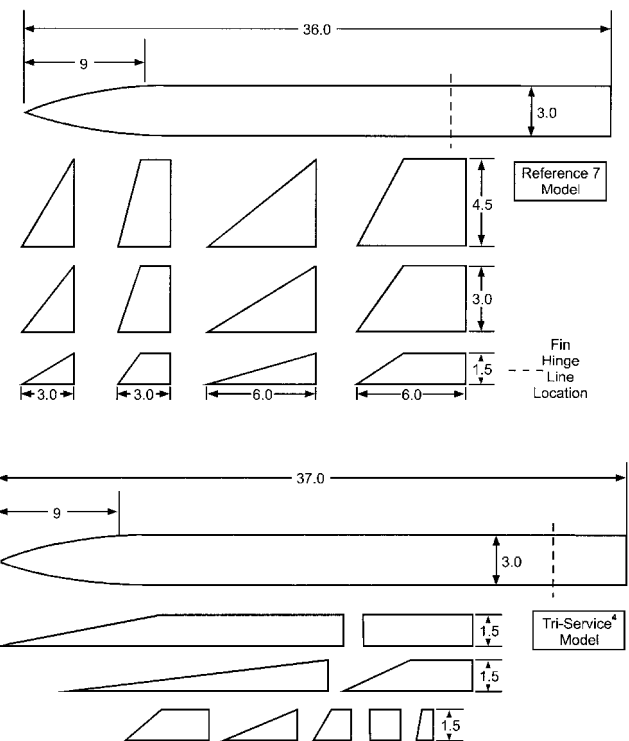


Fig. 2 Scaled geometry comparison with Tri-Service model⁴ and Ref. 7 model (all dimensions in inches).

this mount arrangement apparently caused measurement errors at some conditions. Finally, only two fins were mounted on the body in the $\Phi = 0$ deg roll orientation in the Ref. 7 tests, whereas four fins were mounted on the body in the Ref. 4 database and roll angle was varied as well.

In comparing the AP98 to the Ref. 7 database, it was found that there was good agreement between theory and data. The average error on normal force and center of pressure was about 7 and 2% of the body length, respectively.⁸ Although these comparisons are within the desired accuracy levels of ± 10 and $\pm 4\%$ of body length for normal force and center of pressure, respectively, there were some areas where the AP98 accuracy compared to the Ref. 7 database seemed to warrant improvement. These areas were body-alone normal-force coefficient for $M_\infty > 2.75$, body-alone center of pressure in the transonic Mach number region, and the treatment of the linear term of the body-alone normal-force coefficient above $\alpha = 30$ deg. For the wing-alone and total configuration aerodynamics, some slight changes appeared to be needed in the wing-alone aerodynamics and wing-body interference factors.

Modifications to the AP98

Modifications made to the AP98 (as a result of the Ref. 7 wind-tunnel database) to improve the overall prediction of normal force coefficient and, to a lesser extent, center of pressure, will be discussed in this part of the paper. Modifications will be broken down into body-alone, wing-alone, and wing-body interference factors.

Body-Alone Modifications

The present body-alone static aerodynamics are computed using linearized theories at low AOA and a modified version of the Allen Perkins viscous crossflow theory for the nonlinear AOA aerodynamic terms.¹ One of the keys in obtaining accurate aerodynamics is in obtaining accurate values of the critical crossflow Reynolds number and Mach number. These parameters are of primary importance at low Mach number. For Mach number 2.0 and greater, they have little influence on the aerodynamic terms. The AP98 currently uses a value of $Re_C = 1.8 \times 10^5$ and $M_{N_C} = 0.1$ as standard values. However, the user is allowed to change Reynolds number Re_C and M_{N_C} to specified values.

In comparing the AP98 to the body-alone wind-tunnel data of Ref. 7, good agreement in center of pressure and normal force were obtained. Average errors of normal force were less than 6% and center of pressure less than one-fourth caliber or 2% of the body length. These average errors were calculated using optimum values of the critical crossflow Mach number and Reynolds number, which is quite important for $M_\infty \leq 1.2$ comparisons. Reynolds number Re_C was a constant 3.3×10^5 , and M_{N_C} varied from 0 at $M_\infty = 0.6$ to 0.06 at $M_\infty = 0.9$. Also, error values were calculated at each 5-deg AOA at all Mach numbers where data were available. This gave a total of 40 data points, sufficiently large to get a good statistical average error.

In viewing the individual comparisons, it was clear that a couple of minor problems existed, which, if corrected, could improve these average errors somewhat. The first one has to do with the current body-alone methodology for implementing compressibility effects into the nonlinear normal force term. The present methodology for the body-alone aerodynamics in the normal plane is

$$C_{N_B} = C_{N_L} + \eta C_{d_c} \sin^2 \alpha (A_P / A_{ref}) \quad (1)$$

$$x_{CP} = [(x_{CP})_L C_{N_L} + (x_{CP})_{NL} C_{N_{NL}}] / C_{N_B} \quad (2)$$

$$C_{M_B} = -C_{N_B} (x_{CP} - x_0) \quad (3)$$

In addition, an empirical table of center of pressure shifts was used for the body alone to partially account for physics not adequately accounted for in the determination of center of pressure. These physics include the following: transonic flow where shock waves

can stand on the body, that the linear theory center of pressure does not stay constant as is presently assumed, and that the center of pressure moves in a parabolic fashion [vs a weighted average as represented by Eq. (2)] from its value at $\alpha = 0$ to the centroid of the planform area at a high AOA, for example, 45 deg.

Three slight changes in the Ref. 1 methodology are being implemented as a result of comparisons to the Ref. 7 database. The first has to do with the value of η , which is the normal force of a circular cylinder of given length-to-diameter ratio to that of a circular cylinder of given length. Likewise, η_0 is the value of η at $M_N = 0$. At present,

$$\eta = [(1 - \eta_0)/1.8]M_N + \eta_0 \quad \text{for } M_N < 1.8$$

$$\eta = 1 \quad \text{for } M_N \geq 1.8 \quad (4)$$

Also, η is automatically set to one if $M_\infty \geq 2.75$. This last condition, where η is automatically set to one, appears not to be necessary. In other words, Eq. (4) is allowed to be the sole determination of the value of η . This change mainly affects normal-force results for conditions just above the cutoff Mach number of 2.75.

The second change implemented as a result of the Ref. 7 database has to do with the empirical table for the center of pressure shifts. Some slight changes were implemented that mainly affect results in the transonic region for lower AOAs. The Ref. 7 database had Mach 0.9 data available, which allowed the results of Ref. 1 to be improved on somewhat. These modified results are given in Ref. 8. They result in some slight improvement in the average center of pressure error for the Ref. 1 database from about 0.25 to 0.2 caliber. The 0.2 caliber error is an average error of about 1.6% of the body length.

The third body-alone change has to do with the way the linear and nonlinear terms of Eq. (1) are treated as α increases above 30 deg. The AP98 methodology assumes

$$C_{N_L} = (C_{N_\alpha})\alpha, \quad \alpha \leq 30$$

$$C_{N_L} = (C_{N_L})_{\alpha=30} [1 - (\alpha - 30)/60], \quad 30 < \alpha \leq 90 \quad (5)$$

In reality, the linear term does not decay in the fashion of Eq. (5), but is probably more parabolic in nature. A better representation of the physics is, therefore, assumed to be

$$C_{N_L} = (C_{N_\alpha})\alpha, \quad \alpha \leq 30 \text{ deg}$$

$$C_{N_L} = (C_{N_L})_{\alpha=30}, \quad 30 \text{ deg} < \alpha \leq 45 \text{ deg}$$

$$C_{N_L} = (C_{N_L})_{\alpha=30} [1 - (\alpha - 45)/45] \quad 45 \text{ deg} < \alpha \leq 90 \text{ deg} \quad (6)$$

Figures 3 and 4 compare the AP98 methodology to the AP02, which includes the three body-alone changes discussed. Figure 3 is the Ref. 7 database and Fig. 4 is the Ref. 4 database. Results are shown only for Mach numbers above 2.75 because this is the region where the greatest improvements in prediction accuracy are seen. Both normal-force coefficient and center of pressure are given. Note that the revised method, which will be incorporated as a part of the AP02, shows improvement in comparison to both the Ref. 7 and 4 databases. The average 6–7% error for normal force coefficient of the AP98 compared to the Ref. 7 database is reduced to an average error of about 4%. Also, some improvement in the average error comparisons of the Ref. 4 database is obtained, although this error was not calculated.

Wing-Alone Modifications

The wing-alone methodology of Ref. 1 assumed the wing-alone normal force could be predicted from a fourth-order equation in AOA. That is, assuming no wing camber,

$$C_{N_W} = a_1 \alpha_w + a_2 \alpha_w^2 + a_3 \alpha_w^3 + a_4 \alpha_w^4 \quad (7a)$$

$$a_2 = 34.044(C_N)_{\alpha=15\text{ deg}} - 4.824(C_N)_{\alpha=35\text{ deg}} + 0.426(C_N)_{\alpha=60\text{ deg}} - 6.412a_1 \quad (7b)$$

$$a_3 = -88.240(C_N)_{\alpha=15\text{ deg}} + 23.032(C_N)_{\alpha=35\text{ deg}} - 2.322(C_N)_{\alpha=60\text{ deg}} + 11.464a_1 \quad (7c)$$

$$a_4 = 53.219(C_N)_{\alpha=15\text{ deg}} - 17.595(C_N)_{\alpha=35\text{ deg}} + 2.661(C_N)_{\alpha=60\text{ deg}} - 5.971a_1 \quad (7d)$$

The term a_1 of Eq. (7) is the value of wing-alone lift curve slope at $\alpha=0$ given by linear theory. The terms $(C_N)_{\alpha=15\text{ deg}}$, $(C_N)_{\alpha=35\text{ deg}}$, and $(C_N)_{\alpha=60\text{ deg}}$ are values of the wing-alone normal force coefficients at $\alpha=15$, 35, and 60 deg, respectively, defined by the databases of Refs. 5, 6, and 9. Above α_w of 60 deg, extrapolation of the aerodynamics at α_w of 60 deg is used. For more details of the method, the reader is referred to Ref. 10.

The center of pressure of the wing-alone and wing-body normal force is assumed to vary in a quadratic fashion between its linear theory value near $\alpha=0$ and the centroid of the planform area at $\alpha=60$ deg. If A and B are the centers of pressure of the linear and

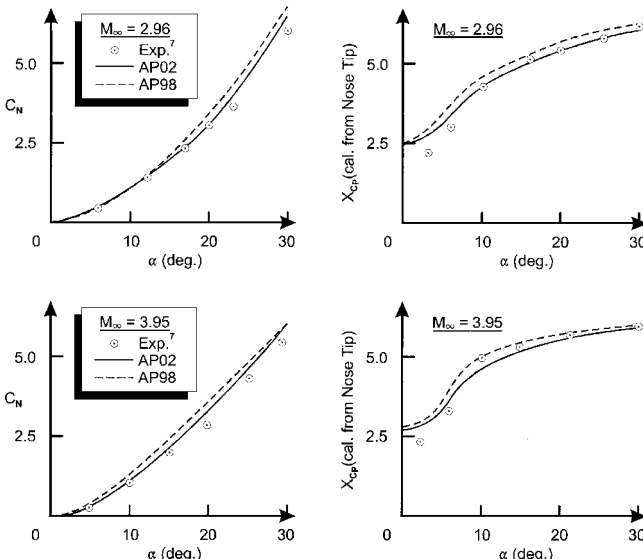


Fig. 3 Comparison of modified body-alone aerodynamics method to experiment for Ref. 7 model of Fig. 2.

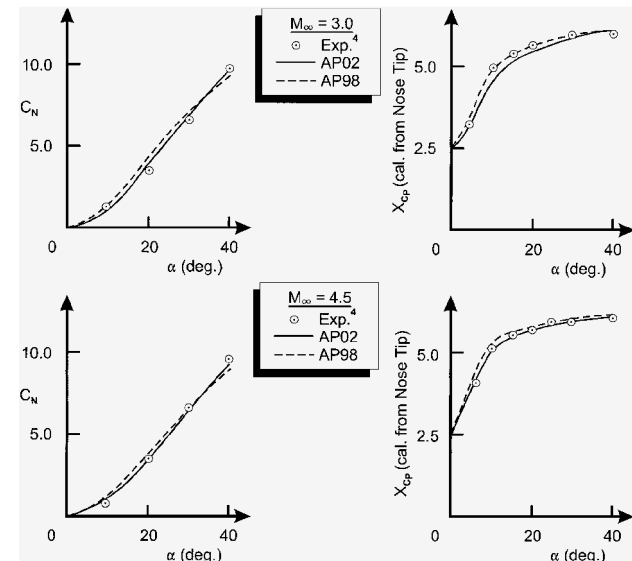


Fig. 4 Comparison of modified body-alone aerodynamics method to experiment for Ref. 4 model of Fig. 2.

nonlinear normal force terms (in percent of mean geometric chord), and $\alpha_w = \alpha + \delta$, then the center of pressure of the wing-body or wing-alone lift is

$$(x_{CP})_{WB} = (x_{CP})_W = A + (1/36)|\alpha_w|(B - A) + (1/5400)\alpha_w^2(A - B) \quad (8)$$

Equation (8) is the methodology used for roll position of 0 deg. For roll position of 45 deg, an equation for a center of pressure shift

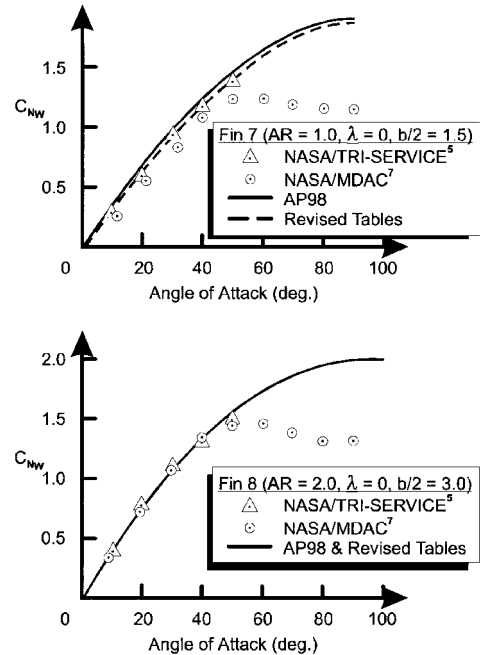


Fig. 5 Comparison of NASA/MDAC⁷ wing-alone database to that of Ref. 5 ($M_\infty = 1.6$).

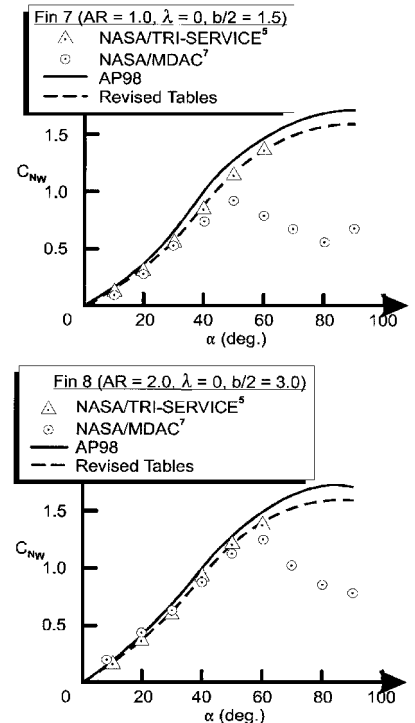


Fig. 6 Comparison of NASA/MDAC⁷ wing-alone database to that of Ref. 5 ($M_\infty = 4.0$).

was derived in Ref. 11 to account for the difference in load on the windward and leeward planes. This shift is added to Eq. (8) for the roll position of $\Phi = 45$ deg and is

$$(\Delta X_{CP})_{WB} = -\{r + [b/(c_r + c_t)](c_r/2 - c_t/3)\} \times \cos(\Phi)^2 \sin(2\alpha)(0.8\alpha/65), \quad \alpha \leq 65 \text{ deg} \quad (9a)$$

$$= -0.8\{r + [b/(c_r + c_t)](c_r/2 - c_t/3)\} \cos \Phi^2 \sin(2\alpha) \quad \alpha > 65 \text{ deg} \quad (9b)$$

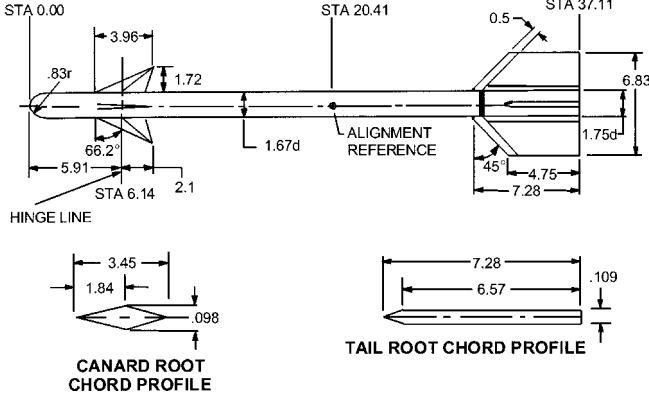


Fig. 7a Canard-body-tail configuration with hemispherical nose.¹⁴

Equations (9a) and (9b) contain a correction to the original center of pressure shift derived in Ref. 11. This change is the square of the $\cos(\Phi)$ term in Eq. (9), whereas in Ref. 11, the $\cos(\Phi)$ term was to the first power. The reason for the square is the fact that the $\cos(\Phi)$ term does two things. First, it rotates the normal force to a plane normal to the body axis as opposed to being normal to the wing. Second, the $\cos(\Phi)$ term rotates the radius vector to the lateral center of pressure of the wing from the Φ roll position to the horizontal plane. Reference 11 omitted this last rotation, causing a slightly more forward center of pressure shift at roll than was warranted. As already mentioned, one of the keys to the Ref. 1 method was the development of the wing-alone normal force coefficient tables for values of α_w of 15, 35, and 60 deg.

The NASA/MDAC⁷ wing-alone database had, in principle, a couple of advantages over the databases used to develop the wing-alone tables at $\alpha = 15, 35$, and 60 deg used in the wing-alone prediction methodology of the AP98 (Ref. 1). First of all, the Ref. 7 database measured wing-alone data for $\alpha = 0$ –90 deg and from $M_\infty = 0.6$ to 4.0. The databases comprising the tables in Ref. 1 consisted of several different sets of data (see Refs. 5, 6, and 9) to cover the Mach number range of interest. In some cases, data from Refs. 5, 6, and 9 was available only to 60-deg AOA, and in some databases the data tended to give a stall effect at higher AOA and so was not useable. On the other hand, data from Ref. 7 was more limited in wing planforms considered than in some of the other databases (Ref. 5, 6, and 9).

As a result of the new database from Ref. 7, it was decided to compare the Ref. 7 database to the AP98 tables as well as the Ref. 5

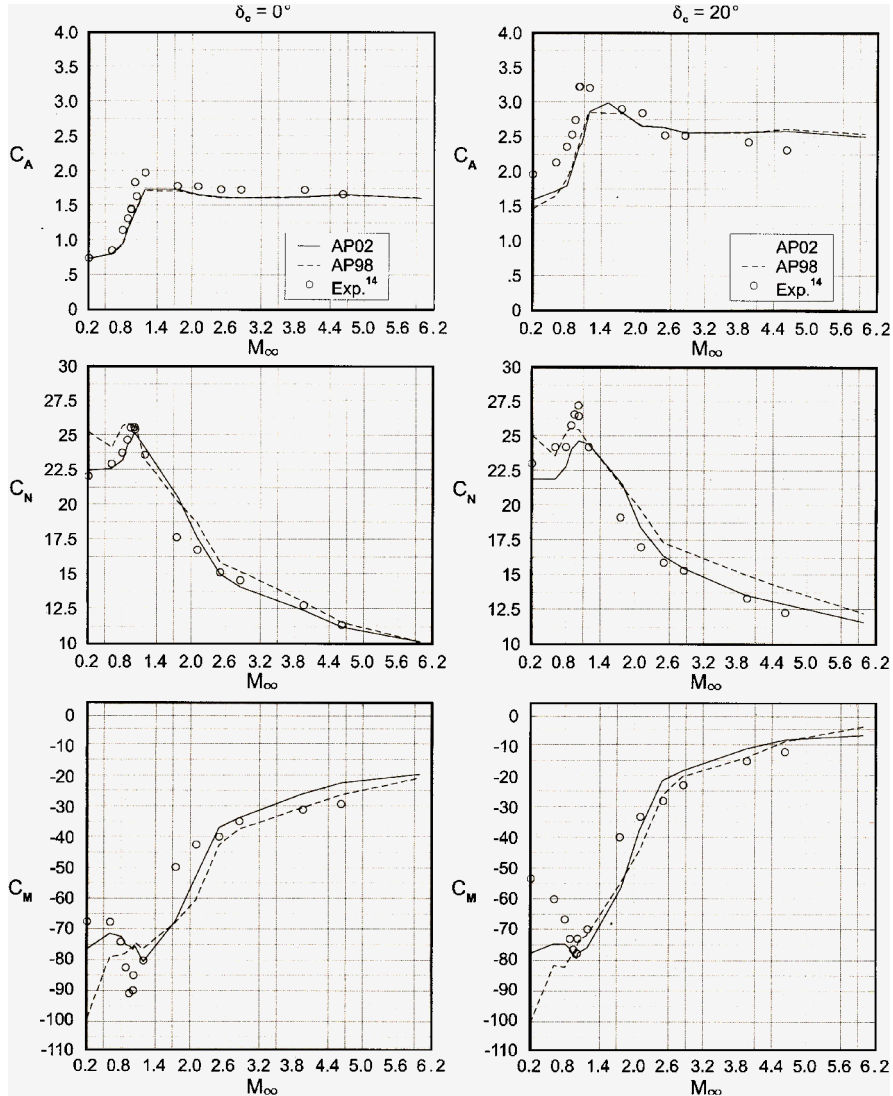


Fig. 7b C_A , C_D , and C_M vs Mach number for configuration of Fig. 7a ($\Phi = 0$ and $\alpha = 20$ deg).

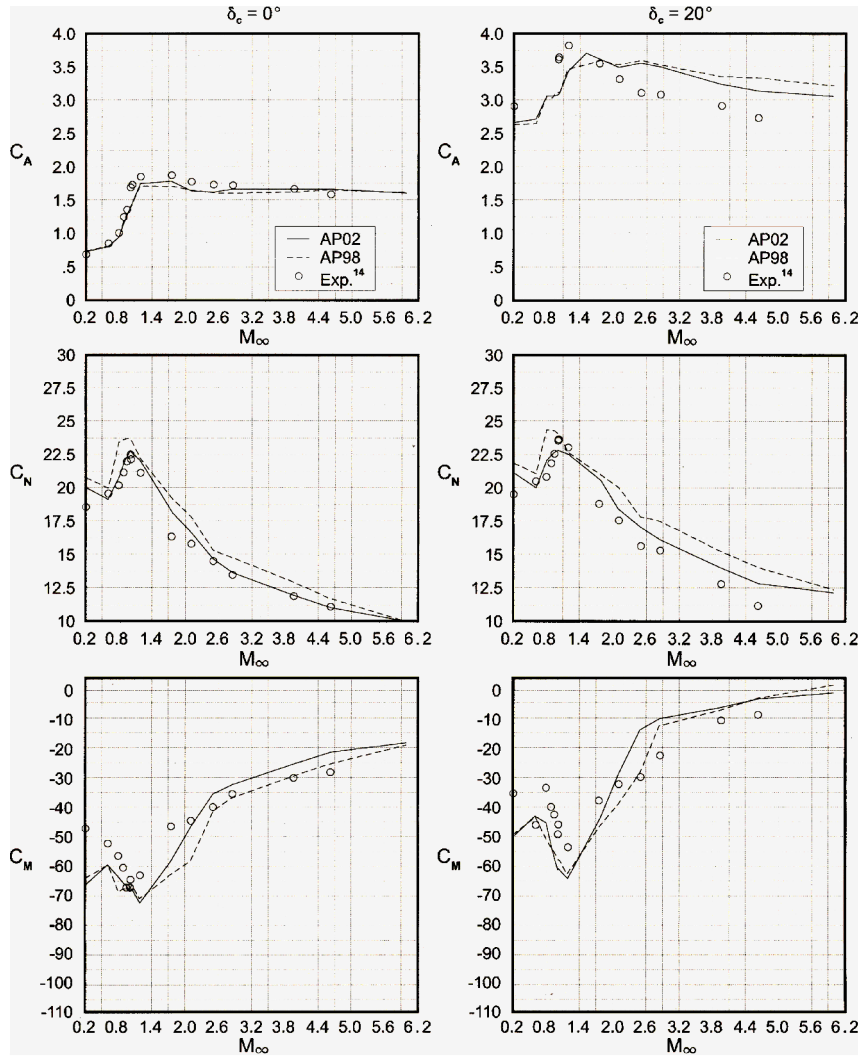


Fig. 7c C_A , C_N , and C_M vs Mach number for configuration of Fig. 7a ($\Phi = 45$ and $\alpha = 20$ deg).

data, which the author still believes is the best wing-alone database available. Comparisons were made as a function of AOA, aspect ratio, Mach number, and taper ratio. Figures 5 and 6 compare the results of the Ref. 5 database and the recent NASA/MDAC⁷ database at Mach numbers of 1.6 and 4.0, respectively, for fins 7 and 8 of Ref. 7. Fin 7 is of aspect ratio 1.0 with taper ratio 0, and has a semispan of 1.5 in., whereas fin 8 is of aspect ratio 2, taper ratio 0, and semispan 3.0 in. Also shown in Figs. 5 and 6 are the results from the AP98 method and revisions to the wing-alone tables to be incorporated in the AP02. Several points are worthy of note. First of all, at both $M_\infty = 1.6$ and 4.0, the Ref. 7 and 5 data are in excellent agreement for fin 8 up to AOA of 40–45 deg. Above $\alpha = 45$ deg, the Ref. 7 data stalls. Also, the Ref. 7 data is consistently about 10% lower than the Ref. 5 data for fin 7 at $M_\infty = 1.6$ and 4.0. It is theorized that because the Ref. 7 data were taken with a splitter plate and Ref. 5 with a sting, the differences in the data are due to the measurement. It is suspected that for the lower semispan, boundary-layer buildup ahead of the fin on the splitter plate is the source of the 10% lower value of C_{Nw} of Ref. 7 data compared to Ref. 5. In other words, for small-span wings, the lower dynamic pressure due to the boundary layer near the root chord has more of an effect than for the larger-span wings. This effect is magnified for small taper ratios because the wing cross-sectional area is the largest at the root chord. It is not known why the flow stalls above about 45 deg for the splitter plate results. However, this was the case for most of the Ref. 7 results. As a result of these two phenomena, it was decided to use considerable judgement before using any of the Ref. 7 results for the 1.5-in. semispan or for any span above $\alpha = 45$ deg. The final point to be made in viewing Figs. 5 and 6 is that the revised values of C_{Nw} , which will be incorporated into the AP02, are

closer to the Ref. 5 data than the AP98. The AP98 had intentionally increased the values of C_{Nw} somewhat to account for the Ref. 5 data having been taken on fairly thick wings to accommodate many pressure taps. It was theorized that these thick wings would lower C_{Nw} unrealistically. The revised data decreases this thickness penalty and is, therefore, much closer to the Ref. 5 data. Other values of revised wing-alone normal force coefficients are given in Ref. 8.

Although not shown in this paper, the slightly lower revised values of C_{Nw} had a slightly adverse impact on the prediction accuracy of the axial force term due to control deflection. As a result, the factor that is used in the AP98 to partially account for some of the nonlinearities that occur due to internal shock interactions when the control surfaces are deflected was also revised. This factor only affects the axial force term due to control deflection when the Mach number is greater than about 2.0.

Refinements For Wing-Body and Body-Wing Interference Factor Nonlinearities

This part of the paper will consider refinements in the empirical factors used to model the nonlinearities in the wing-body and body-wing interference factors due to AOA. No changes will be made in the nonlinear empirical constants associated with the interference factors due to control deflection because the Ref. 7 database did not consider control deflections as a major parameter. Also, the focus here will be on the roll orientation of $\Phi = 0$ deg (fins in plus + roll orientation). The $\Phi = 0$ deg roll emphasis is driven by the Ref. 7 database only having $\Phi = 0$ deg data available. However, when changes are made in the empirical constants for $\Phi = 0$ deg,

the constants for $\Phi = 45$ deg will be considered for change in a complementary way to the $\Phi = 0$ deg results.

To better understand the interference lift components, it is instructive to examine the total normal force of a configuration as defined by Pitts et al.¹² This is given by

$$C_N = C_{N_B} + [(K_{W(B)} + K_{B(W)})\alpha + (k_{W(B)} + k_{B(W)})\delta_W](C_{N_\alpha})_w + [(K_{T(B)} + K_{B(T)})\alpha + (k_{T(B)} + k_{B(T)})\delta_T](C_{N_\alpha})_T + C_{N_{T(V)}} + C_{N_{B(V)}} \quad (10)$$

The first term in Eq. (10) is the normal force of the body alone, including the linear and nonlinear components; the second term is the contribution of the wing (or canard), including interference effects and control deflection; the third term is the contribution of the tail, including interference effects and control deflection; and the last terms are the negative downwash effect on the tail or body due

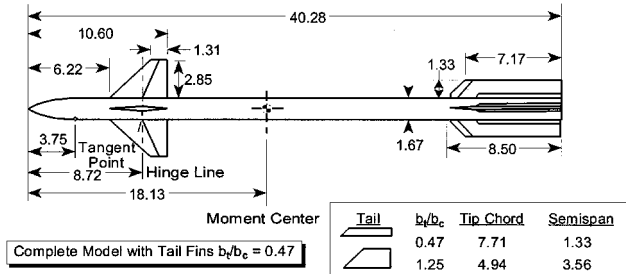


Fig. 8a Canard-body-tail configuration with varying tail span (from Ref. 15) (all dimensions in inches).

to wing-shed or body-shed vortices. The K represent the interference of the configuration with respect to AOA, and the k represent the interference with respect to control deflection. Each of these interference factors is estimated by slender body or linear theory. As such, they are independent of AOA.

The terms that will be considered in this paper for refinements are $K_{W(B)}$, $K_{B(W)}$, $K_{T(B)}$, and $K_{B(T)}$. These four interference factors are defined in the general form

$$K = K_{\text{SBT}} + \Delta K(M_\infty, \alpha, \mathcal{R}, \lambda, \Phi) \quad (11)$$

The first term of Eq. (11) is defined by linear theory or slender body theory, whereas the second term is defined by utilizing several large wind-tunnel databases to back out the nonlinearities as a function of Mach number, AOA, aspect ratio, and taper ratio. The second term of Eq. (11) is defined by 20 tables of empirical data in Ref. 8 as a function of M_∞ , α , \mathcal{R} , λ , and Φ . Both $\Delta K_{W(B)}$ and $\Delta K_{B(W)}$ are defined in this way. Whereas the Ref. 7 data required some changes in these 20 tables compared to the AP98 empirical tables of Ref. 1, the changes in general were minor for most of the tables. The tables are fairly lengthy and will not be shown here, but the interested reader can find them in Ref. 8.

Comparison of Modified Theory (AP02) to Missile Component Databases

The first thing one does after making changes to the APC is to compare the new predictions to the database on which the changes were based in a comprehensive fashion. The database of Ref. 7 consists of Mach numbers 0.6, 0.9, 1.2, 1.6, 2.0, 2.3, 2.96, and 3.95 for the 12 wing-body cases at the top of Fig. 2 and at $\Phi = 0$ deg roll. AOA from 0 to 20 deg were considered at the subsonic and transonic Mach numbers, whereas AOA to 30 deg were considered

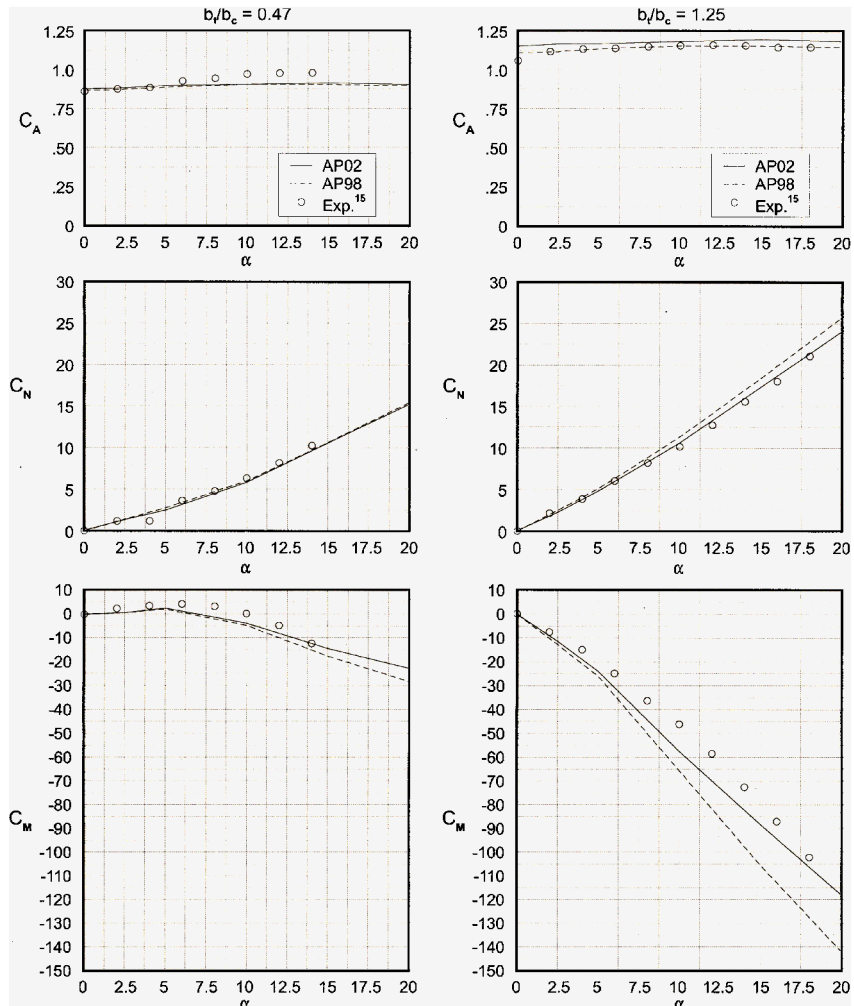


Fig. 8b Comparison of theory and experiment for configurations of Fig. 8a ($\Phi = 45$ deg and $M_\infty = 2.5$).

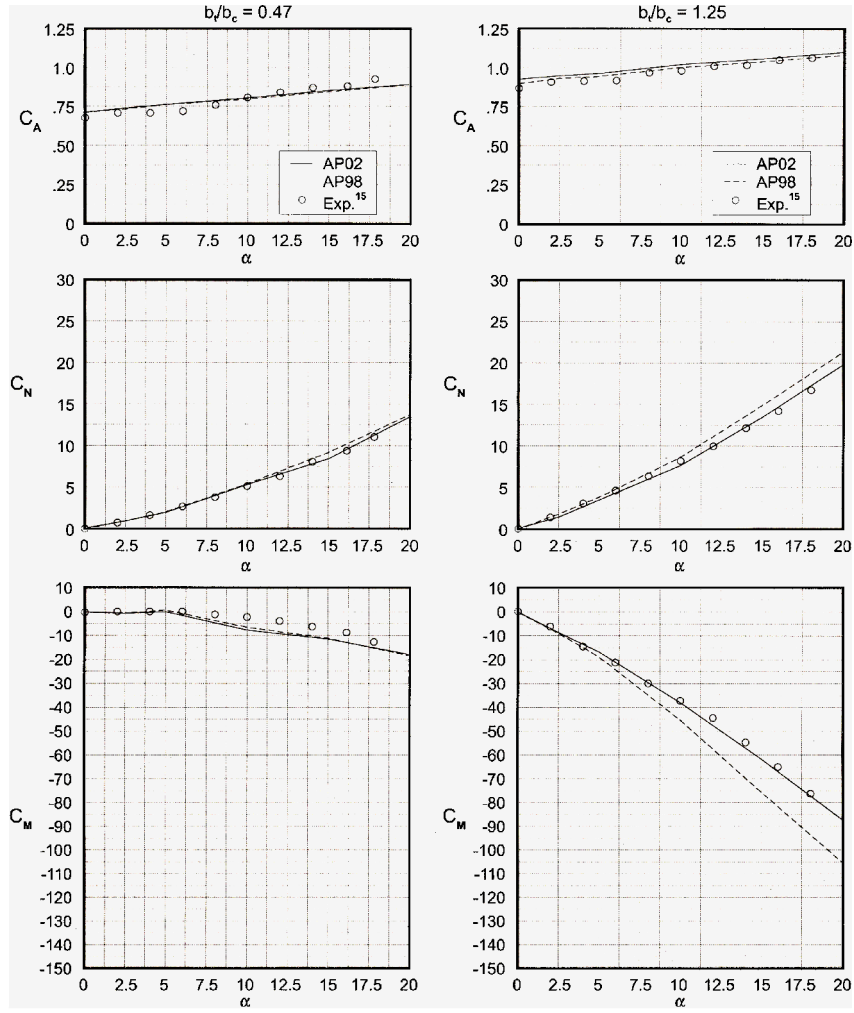


Fig. 8c Comparison of theory and experiment for configurations of Fig. 8a ($\Phi = 45$ deg and $M_\infty = 3.5$).

at the supersonic conditions. In a quantitative sense, the errors of the AP02 compared to experiment were measured at $\alpha = 10, 15, 20, 25$, and 30 deg where data were available. The error here is defined by

$$\text{Error}(\%) = \frac{|C_{N\text{exp}} - C_{N\text{theory}}|}{C_{N\text{exp}}} \times 100 \quad (12)$$

These errors were then averaged by individual Mach number and for all Mach numbers for the 12 fins of the Ref. 7 database. These results are shown in Table 1. As seen in Table 1, the average errors on normal-force coefficient prediction are less than 10% for any Mach number and under 5% for the entire database. Although not shown, the average total error for the AP98 on normal force is closer to 7%. Although this is still under the quoted average error of $\pm 10\%$, it is considerably higher than that given by the improvements that will be part of the AP02.

To check and see whether the AP02 improvements have a positive or negative impact on predictions for the aerodynamics of the NASA Tri-Service database,⁴ Tables 2 and 3 were prepared. The Tri-Service database consisted of Mach numbers 0.6, 0.8, 1.2, 1.5, 2.0, 2.5, 3.0, 3.5, and 4.5 with AOA up to 25–40 deg, depending on Mach number. Fins and body tested are shown at the bottom of Fig. 2. The highest aspect ratio fins were very small ($\mathcal{A} = 4$), and so the data associated with those fins was not considered in the Table 1 and 2 averages. Also, the $\mathcal{A} = 2.0$ fin data were only considered above $M_\infty = 1.5$ in the averaging process. The overall average error for 442 data points in the $\Phi = 0$ deg roll is 3.4%. This compares to a value between 4 and 5% for the AP98. The $\Phi = 45$ deg roll results are presented in Table 3. Here, 362 data points were considered at the same AOA and Mach numbers as for the $\Phi = 0$ deg roll position. The average normal force error for each Mach number is less than

10% and the overall average for the entire database is 3.5%. Reference 13 shows that the AP98 average accuracy for the $\Phi = 45$ deg roll is 6.2% for C_N and 1.2% of the body length for center of pressure.

Table 4 then combines the results for Tables 1–3 into an overall average. This overall average error is less than 4%, with the worst case averages being in subsonic and transonic flow, where matching the optimum critical crossflow Reynolds number is quite difficult. In scanning over the 1230 data points, it was seen that some worse-case errors can approach 35% in the subsonic region, even when we try to utilize the best crossflow Reynolds number for body-alone results. The flowfield changes when wings are added, so that the best critical crossflow Reynolds number for the body alone may be different than the optimum value for the wing–body. Generally speaking, the worst-case errors at supersonic speeds are at low AOA

Table 1 Average normal-force errors of AP02 compared to NASA/MDAC⁷ database ($\Phi = 0$)

Mach number	Number of points	Average error, %
0.6	42	7.2
0.9	42	8.7
1.2	42	3.7
1.6	60	2.7
2.0	60	3.0
2.3	60	3.1
2.96	60	3.7
3.95	60	4.9
Total	426	4.4

Table 2 Average normal-force errors of AP02 compared to NASA/Tri-Service⁴ database ($\Phi = 0$)

Mach number	Number of points	Average error, %
0.6	25	3.2
0.8	30	4.8
1.2	33	3.6
1.5	63	2.2
2.0	59	3.5
2.5	58	2.6
3.0	58	3.7
3.5	57	3.9
4.5	59	3.6
Total	442	3.4

Table 3 Average normal-force errors of AP02 compared to NASA/Tri-Service⁴ database ($\Phi = 45$ deg)

Mach number	Number of points	Average error, %
0.6	22	4.8
0.8	23	7.5
1.2	27	3.8
1.5	49	3.0
2.0	49	3.5
2.5	48	2.5
3.0	49	3.2
3.5	46	3.7
4.5	49	2.7
Total	362	3.5

Table 4 Average normal-force errors of AP02 compared to combined databases^{4,7}

Mach number	Number of points	Average error, %
0.6	89	5.5
0.8-0.9	95	7.2
1.2	102	3.7
1.5-1.6	172	2.6
2.0	168	3.3
2.3-2.5	166	2.8
2.96-3.0	167	3.6
3.5-3.95	163	4.2
4.5	108	3.2
Total	1230	3.8

where experimental data corrections for nonzero AOA were not made. Errors as high as 15% were seen. However, errors of this magnitude for a single data point were quite rare. It is seen that the improvements based on the Ref. 7 database carried over to the Ref. 4 database as well. Hence, the overall average accuracy of the AP02 in predicting lifting characteristics of missile configurations should be slightly improved over the AP98.

No average error on center of pressure was made because of time constraints. However, suffice it to say that the average center of pressure error for the AP98 on the NASA Tri-Service database was less than 2% of the body length.¹³ Improvements made in normal force should only improve these already excellent predictions. Likewise, no improvements in axial force at zero control deflection were sought, as we were quite happy with the power-off predictions of axial force from the AP98. Improvements in power-on axial force will be addressed in a future task.

Comparison of AP02 to Configurations Outside the Refs. 4 and 7 Databases

Although the average accuracy comparisons of C_N to experiment of Tables 1-4 are impressive for a semiempirical code, the true measure of success is based on the ability to accurately predict aerodynamics on a wide variety of configurations outside the databases on which the empirical nonlinearities were derived. Reference 8

considered nine cases over a variety of flight conditions to make the determination of whether the improvements added to the AP02 were generically applicable to other missile configurations and if they improve the accuracy of aerodynamic estimation over the AP98. Only three of those nine cases will be shown here. The three cases selected will be cases where the AP02 improvements showed the largest average normal-force coefficient improvements compared to the AP98 and experimental data. The AP02 showed slight improvement in the other six cases not shown in this paper but given in Ref. 8. The reader is referred to Ref. 8 for these results.

The first configuration considered is taken from Ref. 14 and is a canard-body-tail missile configuration. It is 22.2 calibers in length, and the nose is hemispherical. The tail surfaces are fairly large, with $AR = 0.87$, and fairly thick, with truncated trailing edges. The canards have an $AR = 1.73$. The configuration is shown in Fig. 7a. The hangers that are on the wind-tunnel model were not modeled by the APC. Tests were conducted for $M_\infty = 0.2-4.63$, AOA of 0-20 deg, control deflections of 0-20 deg, roll of 0-45 deg, and $Re/ft = 2 \times 10^6$ for a model with boundary-layertrips. Base pressure values as a function of M_∞ and AOA were given in Ref. 14, and these values were added to the axial force information so that total axial force values could be shown.

Note that the tail thickness in Fig. 7a is less than that of Fig. 32a in Ref. 1. Reference 1 incorrectly used the value of 0.236 in. for the tail thickness, vs the correct value of 0.109 in. as shown in Fig. 7a. This larger value of thickness was the primary source of the overprediction in axial force coefficient in Ref. 1 using the AP98. The correct value of tail thickness was used for both the AP98 and AP02 computations in this paper.

Figure 7b gives the comparison of theory and experiment for $\Phi = 0$ deg roll for both 0- and 20-deg control deflections. Results are shown in terms of C_A , C_N , and C_M (where C_M is about the alignment reference point of Fig. 7a) vs Mach number for $\alpha = 20$ deg. Viewing Fig. 7b, it is seen that the AP98 and AP02 both give good agreement to data. In comparing the AP02 to the AP98 and experiment, it is seen that the AP02 shows some improvement in prediction of normal-force and pitching moment coefficients compared to the AP98 for 1) Mach numbers less than 0.9 and 2) Mach numbers greater than 2.1 for normal-force coefficient. For the intermediate Mach numbers, prediction accuracy of the two versions of the APC is comparable. Axial force prediction accuracy for this configuration of the two codes is also comparable because only minor changes were made to the AP02 with respect to axial force estimation.

The $\Phi = 45$ deg roll comparisons of C_A , C_N , and C_M for $\alpha = 20$ deg and $\delta_C = 0$ and 20 deg are shown in Fig. 7c. In general, the AP02 gives better normal-force coefficient predictions compared to data than does the AP98. Pitching moment coefficients predicted by the AP02 are also slightly better than those predicted by the AP98, although the improvement is not as great as for the normal-force coefficient. Again, little difference in axial force coefficient is seen between the AP02 and AP98.

To summarize the first validation case presented here, it is seen that the improvement in normal-force prediction accuracy of the AP02 based on the more recent database of Ref. 7 carried over to the Fig. 7a configuration. For the 56 data points of Figs. 7b and 7c (14 Mach numbers, 2 roll orientations, and 2 control deflections), the average normal-force error was reduced from 7.9% using the AP98 to 4.2% using the AP02. This is a reduction in the normal-force prediction error of over 40%. Some slight improvement in pitching moment, center of pressure, and axial force was also observed for the AP02 compared to the AP98. However, these improvements were not nearly as large as for normal-force coefficient.

The second case shown here in the evaluation of the improved empirical constants developed for the nonlinear aerodynamic terms of the normal force coefficient is taken from Ref. 15 and is shown in Fig. 8a.

The wind-tunnel model was about 22 calibers in length with a sharp nose of 2.25 calibers. The canards had an aspect and taper ratio of 2.0 and 0.3, respectively. Various tail fin spans were considered. This model was tested at Mach numbers 1.6-3.5 at AOA to about

18–20 deg. It had a boundary-layer trip present and was tested at $Re/ft = 2.0 \times 10^6$. Reference 15 gave separate values of base axial force coefficient, which were added to the axial force values given in the reference to compare to the AP98 and AP02 computations. To compare the experimental data to theory, Mach numbers of 2.5 and 3.5 are selected at roll angle 45 deg. Also, values of the tail-to-canard semispan of 0.47 and 1.25 are considered. Figures 8b and 8c present the comparison of theory to experiment for $b_t/b_c = 0.47$ and $b_t/b_c = 1.25$ at Mach numbers of 2.5 and 3.5, respectively, for C_A , C_N , and C_M .

In examining Figs. 8b and 8c, it is seen that the AP02 and AP98 both give excellent agreement with experiment for the $b_t/b_c = 0.47$ case. However, for the $b_t/b_c = 1.25$ case, the AP02 shows significant improvement over the AP98 in both C_N and C_M at both $M = 2.5$ and 3.5. Average normal-force coefficient and center of pressure errors were reduced by a factor of two or more for this case, with the AP02 compared to the AP98 and experiment.

The last case considered here is shown in Fig. 9, and the test data were given in a report by Howard and Dunn.¹⁶ This configuration has dorsals that have an $\mathcal{R} = 0.12$ and tail surfaces that have an $\mathcal{R} = 4.0$. The exact configuration illustrated at the top of Fig. 9 is not within the allowable constraints for fin planform required by the APC. Therefore, a modified version of the fin planforms is required, one that meets the constraints of the APC. This configuration is shown in the middle of Fig. 9. Note that the parameters that were held constant for the fin planforms were area, aspect ratio, span, taper ratio, leading-edge sweep angle, and location of the geometric centroid of the planform area. The Howard and Dunn¹⁶ work gave only normal force as a function of AOA. The AP02 and AP98 results are also shown at the bottom of Fig. 9. Quite acceptable agreement is

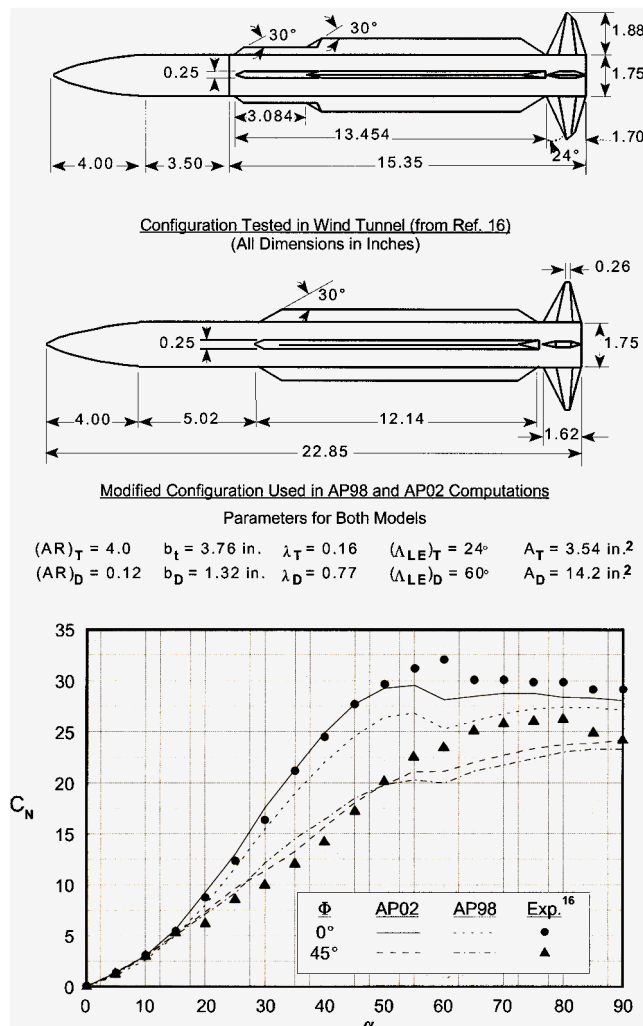


Fig. 9 Normal-force coefficient comparison of theory and experiment ($M_\infty = 0.1$).

obtained with the AP02 compared to experiment, even at high AOA. The AP98 and AP02 are somewhat lower than the data suggest at high α . However, part of this underprediction is suspected to be the tendency of a base-mounted sting to give larger-than-true normal forces at subsonic Mach numbers.^{17,18} In making this statement, sting interference effects were assumed to be unaccounted for in Ref. 16. When we compare the results of the AP02 to the AP98 in a quantitative sense, the average normal force error of the AP98 for 34 data points is 10.7%, whereas the average normal force error of the AP02 is 6.0%. This 6.0% error is based on 34 data points at both the $\Phi = 0$ and 45 deg roll orientations.

Summary and Conclusions

To summarize, the nonlinear empirical constants used in the APC to predict nonlinear normal force and pitching moments on missile configurations at high AOA have been refined based on a more recent missile-component, wind-tunnel database.⁷ In addition, some minor improvements in body-alone normal force and center of pressure have been made. In comparing the new aerodynamic predictions of the revised code (AP02) to the latest released version of the APC (AP98) the following conclusions were drawn:

1) The refined nonlinear empirical coefficients reduced the average normal-force error of the AP02 compared to the AP98 for the NASA/MDAC⁷ database by over a third (7.0% average to 4.4% average error based on 426 data points)

2) In comparing the new AP02 to the AP98 for the older NASA Tri-Service database,⁴ it was seen that the improvements made to the empirical constants also gave improvements in accuracy of normal force coefficient for this database as well. Average normal force errors were reduced from 4–5% for the AP98 to 3.4% for the AP02. This also represents close to a one-third reduction in average normal-force coefficient errors.

3) No quantitative assessment was made of center of pressure (or pitching moment) improvements. However, in viewing the results qualitatively, it is believed that a slight overall improvement was realized by the improved normal-force loads. In addition, an error in the center of pressure shift at roll of 45 deg was corrected in the AP02, also adding some slight improvement in center of pressure predictions.

4) In comparing the AP02 to the AP98 on nine wing-body-tail configurations outside of the missile component databases on which the nonlinear empirical constants were derived, it was found that, in general, the improvements in average normal-force error of the AP02 were seen here as well. The average improvements range from only a slight improvement on one case to over a 40% reduction in error for the best case. Overall, it is guessed that the average normal-force error was reduced by about 20–30% from the AP98 to the AP02.

5) Although the overall accuracy improvement in normal force coefficient is based on averages, one can still find a single data point error on either the AP98 or AP02 where the error is as high as 35%. These worst-case data points usually occur at subsonic or transonic speeds where it is very difficult to predict the correct value of critical crossflow Reynolds number and Mach number.

6) No assessment of axial force errors were made because only minor changes were implemented into the AP02 compared to the AP98.

7) Based on the overall improvement in normal force using the refined nonlinear constants of this report, these improvements will be a part of the next version of the APC that will be transitioned to users in fiscal year 2002.

Acknowledgments

The work described in this report was supported through the Office of Naval Research through the Surface Weapons Systems Technology Program managed at the U.S. Naval Surface Warfare Center, Dahlgren Division (NSWCDD) by Robin Staton. Tasking from this program was provided by Roger Hormann and John Fraysse. Also, some support was provided by the Marine Corps Weaponry Technology Program managed at NSWCDD by Craig Melton. The authors express appreciation for support received in this work.

References

¹Moore, F. G., McInville, R. M., and Hymer, T., "The 1998 Version of the NSWC Aeroprediction Code: Part I—Summary of New Theoretical Methodology," U.S. Naval Surface Warfare Center, Dahlgren Div. TR-98/1, Dahlgren, VA, April 1998.

²Moore, F. G., McInville, R. M., and Robinson, D. I., "A Simplified Method for Predicting Aerodynamics of Multi-Fin Weapons," U.S. Naval Surface Warfare Center, Dahlgren Div. TR-99/19, Dahlgren, VA, March 1999.

³Hymer, T. C., Downs, C., and Moore, F. G., "Users Guide for an Interactive Personal Computer Interface for the 1998 Aeroprediction Code (AP98)," U.S. Naval Surface Warfare Center, Dahlgren Div. TR-98/7, Dahlgren, VA, June 1998.

⁴NASA Langley Research Center Tri-Service Missile Database, transmitted from NASA Langley Research Center by J. M. Allen to U.S. Naval Surface Warfare Center, Dahlgren Div., 5 Nov. 1991 (formal documentation of database in process).

⁵Stallings, R. L., Jr., and Lamb, M. L., "Wing-Alone Aerodynamic Characteristics for High Angles of Attack at Supersonic Speeds," NASA TP 1989, July 1981.

⁶Baker, W. B., Jr., "Static Aerodynamic Characteristics of a Series of Generalized Slender Bodies With and Without Fins at Mach Numbers from 0.6 to 3.0 and Angles of Attack from 0 to 180°," Arnold Engineering Development Center, TR-75-124, Vols. 1 and 2, Tullahoma, TN, May 1976.

⁷Allen, J. M., Hemsch, M. J., Burns, K. A., and Oeters, K. J., "Parametric Fin-Body and Fin-Alone Database on a Series of 12 Missile Fins," NASA Langley Research Center TM (to be published).

⁸Moore, F. G., and McInville, R. M., "Refinements in the Aeroprediction Code Based on Recent Wind Tunnel Data," U.S. Naval Surface Warfare Center, Dahlgren Div. TR-99/116, Dahlgren, VA, Dec. 1999.

⁹Nielsen, J. N., Hemsch, M. J., and Smith, C. A., "A Preliminary Method for Calculating the Aerodynamic Characteristics of Cruciform Missiles to High Angles of Attack Including Effects of Roll Angle and Control Deflections," Office of Naval Research, ONR-CR215-216, 4F, Arlington, VA, Nov. 1977.

¹⁰Moore, F. G., and McInville, R. M., "A New Method for Calculating Wing Alone Aerodynamics to Angle of Attack 180°," U.S. Naval Surface Warfare Center, Dahlgren Div. TR-94/3, Dahlgren, VA, March 1994.

¹¹Moore, F. G., and McInville, R. M., "Extension of the NSWCDD Aeroprediction Code to the Roll Position of 45 Degrees," U.S. Naval Surface Warfare Center, Dahlgren Div. TR-95/160, Dahlgren, VA, Dec. 1995.

¹²Pitts, W. C., Nielsen, J. N., and Kaatari, G. E., "Lift and Center of Pressure of Wing-Body-Tail Combinations at Subsonic, Transonic, and Supersonic Speeds," NACA TR 1307, 1957.

¹³Moore, F. G., McInville, R. M., and Hymer, T., "The 1995 Version of the NSWC Aeroprediction Code: Part I—Summary of New Theoretical Methodology," U.S. Naval Surface Warfare Center, Dahlgren Div. TR-94/379, Dahlgren, VA, Feb. 1995.

¹⁴Graves, E. B., and Fournier, R. H., "Stability and Control Characteristics at Mach Numbers From 0.20 to 4.63 of a Cruciform Air-to-Air Missile With Triangular Canard Controls and a Trapezoidal Wing," NASA TMX 3070, May 1974.

¹⁵Blair, A. B., Jr., Allen, J. M., and Hernandez, G., "Effect of Tail-Fin Span on Stability and Control Characteristics of a Canard Controlled Missile at Supersonic Mach Numbers," NASA TP 2157, June 1983.

¹⁶Howard, R. M., and Dunn, A., "Missile Loads at High Angles of Attack," *Journal of Spacecraft and Rockets*, Vol. 28, No. 1, 1991, pp. 124, 125.

¹⁷Dietz, W. E., Jr., and Altstatt, M. C., "Experimental Investigation of Support Interference on an Ogive Cylinder at High Incidence," *Journal of Spacecraft and Rockets*, Vol. 16, No. 2, 1979, pp. 67, 68.

¹⁸Canning, T. N., and Nielsen, J. N., "Experimental Study of the Influence of Supports on the Aerodynamic Loads on an Ogive Cylinder at High Angles of Attack," AIAA Paper 81-0007, Jan. 1981.

M. S. Miller
Associate Editor